coatings

MDPI

Article

Enhancing the Corrosion Resistance of ZnAl-LDHs Films on AZ91D Magnesium Alloys by Designing Surface Roughness

Xiaoge Wang [1,2], Luchun Yan [1,*], Kewei Gao [1,*], Pengcheng Li [3] and Jiujiu Hao [2]

[1] School of Materials Science and Engineering, University of Science and Technology Beijing, Beijing 100083, China
[2] Department of Metallurgical Engineering, Shanxi Engineering Vocational College, Taiyuan 030009, China
[3] College of Mechanical and Vehicle Engineering, Taiyuan University of Technology, Taiyuan 030024, China
* Correspondence: y_luchun2023@163.com (L.Y.); gaokw_hls@yeah.net (K.G.)

Abstract: Zinc–aluminum layered double hydroxides (ZnAl-LDHs) film is a typical effective corrosion resistant film currently being explored. In this study, ZnAl-LDHs film was prepared on magnesium alloys with different surface roughness by means of metallographic preparation combined with the hydrothermal method. When the surface roughness S_a was at a minimum of 0.094 μm, the ZnAl-LDH films grew the most intensely, reaching 3.8 μm in thickness with a static contact angle of 84.34° and a minimum corrosion current density (i_{corr}) of 1.12×10^{-4} A/cm^2. After the neutral salt spray test, the sample mass was only increased by 0.0424 g. The results show that the size of ZnAl-LDHs nanosheets can be tailored by roughness of Mg alloy surface. The low roughness of magnesium substrate can accelerate the growth rate of ZnAl-LDH films, increase the thickness of films, and improve their corrosion resistance, but it is disadvantageous to the excellent hydrophobic properties of the surface. Finally, the possible growth and corrosion prevention mechanisms of LDHs films were proposed. This also provides a theoretical basis for the optimal processing parameters of magnesium alloy surface.

Keywords: surface roughness; ZnAl-LDHs; corrosion resistance; magnesium alloys

check for updates

Citation: Wang, X.; Yan, L.; Gao, K.; Li, P.; Hao, J. Enhancing the Corrosion Resistance of ZnAl-LDHs Films on AZ91D Magnesium Alloys by Designing Surface Roughness. *Coatings* **2023**, *13*, 724. https://doi.org/10.3390/coatings13040724

Academic Editor: Stefano Rossi

Received: 26 February 2023
Revised: 28 March 2023
Accepted: 29 March 2023
Published: 2 April 2023

Copyright: © 2023 by the authors. Licensee MDPI, Basel, Switzerland. This article is an open access article distributed under the terms and conditions of the Creative Commons Attribution (CC BY) license (https://creativecommons.org/licenses/by/4.0/).

1. Introduction

An important means to reduce energy consumption and pollutant emissions is to make products "lightweight" [1,2]. Magnesium alloys, among various light alloys, have excellent strength-to-weight ratios, high shock absorption, and high recyclability and have become a research hotspot in the last 10 years [3–5]. However, due to the low standard electrode potential (−2.37 V) of magnesium, the oxide film formed by oxidation under natural conditions cannot effectively protect the matrix [6,7]. In particular, when in contact with other metals, magnesium alloys are always severely corroded as the anode of the corrosion couple, greatly restricting the widespread application of magnesium alloys in the industry [8,9]. Thus, developing high corrosion-resistant surface treatment technology has historically been an important way to improve the service life of magnesium alloys [10].

Layered double hydroxides (LDHs), as a member of the two-dimensional material family, incorporate many advantages, especially with their flexible composition and inherent anion exchange performance, which gives them intrinsic protective benefits in the high chlorine marine environment [11,12]. Therefore, many researchers have made great efforts to prepare LDH films on the surface of magnesium alloys to enhance their corrosion resistance [13–16]. The most commonly used preparation method is in situ growth, which is due to the strong bond between the films and the substrate obtained by this method [17,18]. However, it was found that the growth of LDH films was closely related to the surface roughness of the substrate [19,20]. Li [21] et al. found that the morphology and structure of $Mg(OH)_2$/MgAl-LDH composite films can be controlled to achieve corrosion resistance and biocompatibility of AZ91D magnesium alloys by designing the surface roughness of

different magnesium substrates. Panrecious et al. [22] found that the combination of the rough surface of LDHs films with low surface energy can effectively achieve this characteristic of superhydrophobic substrate and greatly improve the corrosion resistance of the material. Therefore, in order to effectively control the good performance of LDH films, it is necessary to understand the influence of substrate surface state on the growth of LDH films, especially surface roughness. The pretreatment of substrates is not the same in many studies. Zhou [23] and Li [24] et al. pretreated the substrate surface of magnesium alloys with different degrees of step polishing prior to preparation of superhydrophobic antiseptic membranes. Although the pretreatment of the substrate increased the corrosion resistance of magnesium alloys, there was no specific and detailed report on how substrate roughness affected the growth of LDH films.

In order to enable researchers to scientifically and effectively control the growth state of LDH films and construct high/low roughness surfaces during the research process, four magnesium alloy substrates with different surface roughness were designed using metallographic methods. ZnAl-LDH films were prepared on the substrate using hydrothermal methods. The effects of substrate surface roughness on the growth morphology, growth rate, and corrosion resistance of LDH films were discussed. This also provides a theoretical basis for the substrate pretreatment process parameters for preparing ZnAl-LDH films.

2. Materials and Methods

2.1. Materials and Preparations of ZnAl-LDHs Film

AZ91D magnesium alloy plates (wt%: Al 8.9; Zn 0.62; Mn 0.32; Si 0.05; Fe 0.004; Ni 0.001; with balance being Mg) with dimensions of 10 mm × 10 mm × 4 mm were used as substrate material [25]. To clear away the superficial oxide/hydroxides and other possible impurities, and to ensure different surface roughness, the alloy samples were polished with 600#, 1200#, 2000#, and 5000# sandpapers and labeled "600", "1200", "2000", and "5000", respectively, and then put into absolute ethanol for ultrasonic cleaning for 15 min and dried with cold wind. All reagents used in the preparation of the film, i.e., aluminum nitrate, zinc nitrate, and sodium hydroxide, were of analytical grade. The preparation of the film-forming solution was as follows: $Zn(NO_3)_2{\cdot}6H_2O$ (1 M) and $Al(NO_3)_3{\cdot}9H_2O$ (0.5 M) were dissolved in 1 L of degassed distilled water under magnetic stirring vigorously to form a homogeneous solution and then transferred into a Teflon-lined stainless-steel autoclave. The pH value was adjusted to 10~11 by the addition of 2 mol/L NaOH solution. The cleaned Mg sheets were vertically placed in the solution for hydrothermal reaction at 85 °C for 12 h. After the reaction, the Mg sheets were washed with deionized water and dried in air.

2.2. Surface Morphology, Roughness, and Crystallographic Structure Characterizations

A field emission scanning electron microscope (FE-SEM, Zeiss GeminiSEM300, Oberkochen, Germany) was used to investigate the surface morphology of each ZnAl-LDHs film. The energy dispersive X-ray spectrometer (EDS) attached to the SEM was utilized to analyze the content and element distribution qualitatively. The films were coated with gold using a thermal evaporator before imaging to minimize charging problems. The materials' crystallographic structures were studied using an X-ray diffractometer (XRD, Rigaku D/max-rB, Tokyo, Japan) with a Cu target (λ = 0.154 nm, 40 kV, 150 mA) at a scanning rate of 1° min^{-1}, and the data were analyzed using MDI Jade (v6.0, 2019, Materials Data, Livermore, CA, USA) software. The surface roughness was measured with a 3D laser scanning microscope (VK-X, Keyence, Jinan, China), a height resolution of about 10 nm, and a measurement speed (velocity) between 0.1 mm s^{-1} and 0.5 mm s^{-1}. The measured area was 10 mm by 10 mm (stylus method with 2000 × 2000 points). Selected parameters (from ISO 25,178) were taken into account: arithmetic mean height S_a.

Contact angle measurements were performed using the Shanghai Zhongchen (Shanghai, China) JC2000D1 test rig. In order to test the static contact angle, 2 μL of distilled water was collected in droplet form, 3~5 different locations were measured for each of the

samples, and the average was taken as the magnitude of the contact angle. A tape-peel test was performed as per ASTM D3359-17 to evaluate the adhesion strength between the prepared films and substrates. Two vertical scratches made with a special knife (QFHHG600, Guangdong, China) were used to identify the grating patterns. After being pressed onto the cut surface for 120 s, the scotch tape was peeled off.

2.3. Electrochemical and Neutral Salt Spray Tests

The potentiodynamic polarization and electrochemical impedance spectroscopy (EIS) tests on the electrochemistry workstation (PGSTAT302N, Metrohm, Herisau, Switzerland) were proceed at room temperature in 0.1 M NaCl aqueous solution. The classical three-electrode system was adopted. The sample was used as the working electrode (area, 1 cm^2), the Ag/AgCl electrode (saturated with KCl) as the reference electrode, and the platinum sheet as the opposite electrode. The potentiodynamic polarization curves were, subsequently, performed at a potential scanning rate of 1 $mV \cdot s^{-1}$ from -0.5 V to 0.5 V versus open circuit potential. The corrosion potential and corrosion current density were analyzed by Tafel extrapolation theory. EIS tests were performed in the frequency range from 10 mHz to 100 kHz applying 10 mV amplitude perturbation. The experimental EIS plot was fitted to equivalent circuits using the Zview software, maintaining errors of <10% and chi-squared values of <0.01 for individual parameters.

According to GB/T10125-2012, the neutral salt spray test was carried out in a salt spray test chamber (GT-7400-L, China) at 35 °C, a saturated barrel temperature of 47 °C, a spray pressure of 1.0 kg/cm^2, a test solution of (50 $\pm$ 5) g/L NaCl aqueous solution, a pH value of 6.5~7.2, and a spray volume of (1.0~2.0) $mL/(80\ cm^2 \cdot h)$. After the test, the samples at 15°~25° to the vertical direction were rinsed with anhydrous alcohol and dried on filter paper. Three identical samples at the same conditions were used to confirm reproducibility.

3. Results and Discussion

3.1. Surface Roughness Analysis

In order to evaluate the change in surface topography, surface roughness, which was an essential optimizing target, was measured. The three-dimensional morphologies of AZ91D magnesium alloys treated with different processing techniques before and after being coated with ZnAl-LDH films are shown in Figure 1. The surface roughness S_a is a roughness assessment parameter based on the domain topography.

Figure 1a,c,e,g illustrated that the surface of the magnesium alloys after grinding with 600, 1200, 2000, and 5000 sandpapers all showed evident scratches, and then the average surface roughness of each sample was determined from it. The measured values S_a were 0.244, 0.194, 0.152, and 0.094 μm, respectively, i.e., the surface of the sample becomes smoother as the grade of silicon carbide sandpaper increases. Furthermore, after in situ growth of ZnAl-LDH films on the surface of the corresponding ground magnesium alloy substrate, the surface flatness was enhanced, and the roughness values S_a were decreased to 0.228, 0.185, 0.136, and 0.082 μm in turn, as shown in Figure 1b,d,f,h. This indicated that the growth of ZnAl-LDH films on the substrate can reduce the roughness of the original substrate surface, and the surface roughness value S_a was inversely proportional to the degree of grinding.

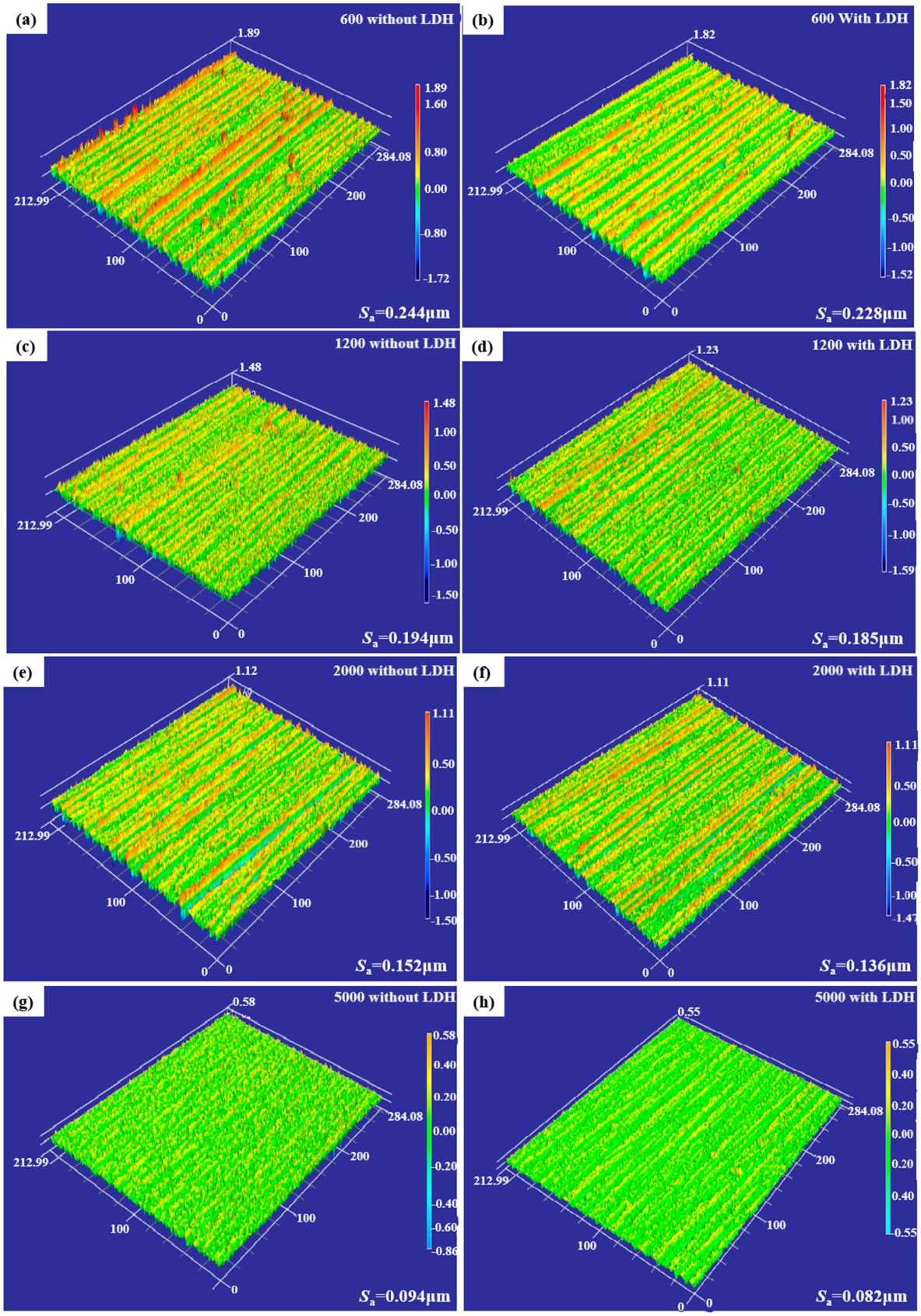


Figure 1. Surface roughness images of magnesium alloy substrates without and with ZnAl-LDH films: (**a**,**b**) 600; (**c**,**d**) 1200; (**e**,**f**) 2000; and (**g**,**h**) 5000.

3.2. Microstructure Analysis

The SEM morphologies and related EDS spectra of ZnAl-LDH films grown on substrates with different roughness are plotted in Figure 2. The different surface roughness of the substrates has a great influence on the growth morphology of the films. Figure 2a–d shows the typical flake-like nanosheets of LDH films. It is worth noting that the surface with high roughness has some protrusions in the whole film layer, and the grown LDH nanosheets are more sparsely distributed and smaller in size. As the surface roughness value S_a decreases, the size of LDH nanosheets gradually increases, and the films become denser. This may be because the magnesium matrix with high surface roughness has a large surface area and more grain boundaries, and the grain boundaries and grain positions formed by protrusions are different, which provide more nucleation sites for the growth of ZnAl-LDHs, resulting in different Mg dissolution rates and ZnAl-LDH film nanosheet growth rates, and thus different film thicknesses at corresponding locations [26]. In order to better compare the content of each element in the films, the carbon measurement peaks are hidden from the EDS analysis. The position of the point scan is marked in red. The results show that the elements composing ZnAl-LDH films are mainly Mg, O, Zn, and Al, indicating the presence of ions suitable for the preparation of LDHs films. The content of Mg^{2+} decreases as the surface roughness S_a decreases because the smoother the surface the smaller the interface for the magnesium matrix to participate in the reaction. However, the ratios of Zn/Mg and Al/Mg are too low, indicating that the in situ growth of the film is thinner, and Mg^{2+} is mainly derived from the Mg matrix.

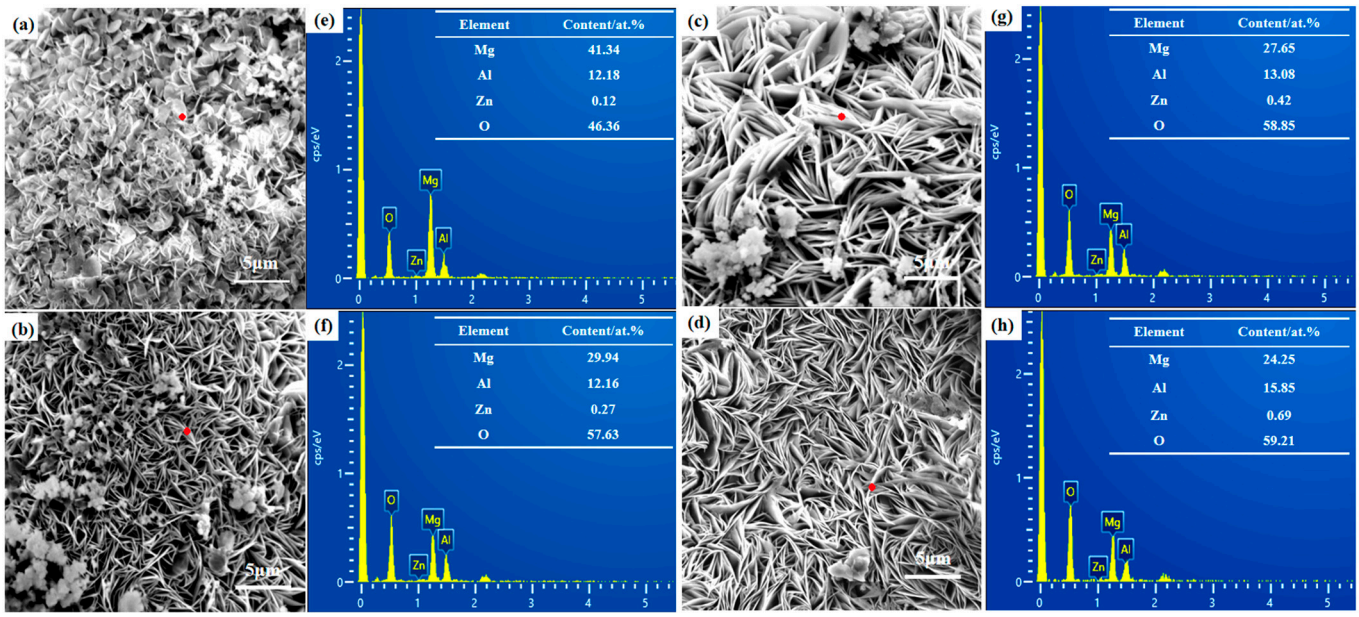


Figure 2. SEM surface micrographs and EDS analysis of ZnAl-LDH films grown on AZ91D Mg alloy with different surface roughness: (**a**,**e**) 600; (**b**,**f**) 1200; (**c**,**g**) 2000; and (**d**,**h**) 5000.

3.3. Crystal Structure Analysis

To further determine the crystalline structure of the ZnAl-LDH films, the XRD patterns results are presented in Figure 3. All XRD spectra has similar evident LDH characteristic diffraction peaks at 11.6° and 23.3°, corresponding to the (003) and (006) planes, respectively, indicating that all samples have a complete layered structure and a good crystal structure. This indicates that matrix roughness does not alter the growth structure of LDH films. According to the Bragg equation, the available surface spacing for d003 is about 0.785 nm. It can be seen from the figure that the LDHs peak intensity of the surface with the smallest roughness value is the largest, which means that the LDHs film grows on this surface with good density. In addition, three relatively strong magnesium alloy diffraction peaks are found in the spectrum, located at 32.4°, 34.7°, and 36.8°, corresponding to the (100), (002),

and (101) planes, respectively. The peaks of the magnesium alloy substrate are all marked with circles. This also indicates that the in situ growth of LDHs films is thinner.

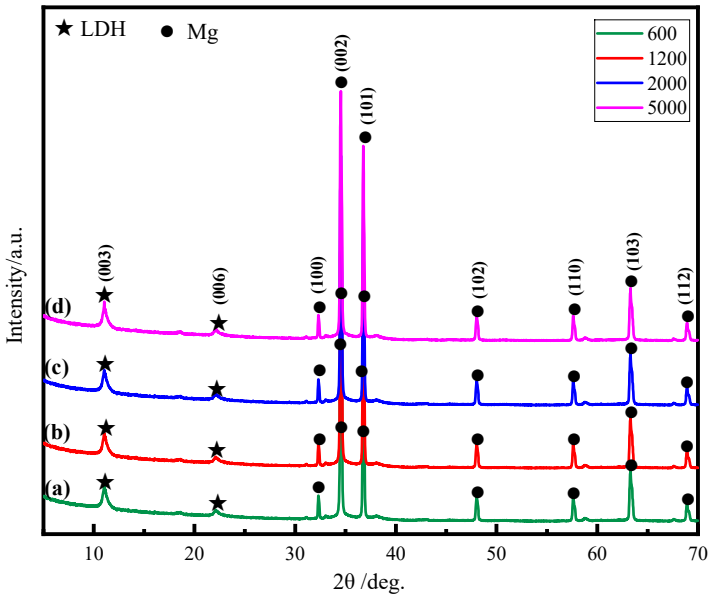


Figure 3. XRD patterns of ZnAl-LDH films grown on AZ91D Mg alloy with different surface roughness: (**a**) 600; (**b**) 1200; (**c**) 2000; (**d**) 5000.

3.4. Cross-Sectional Analysis

The cross-section morphology of ZnAl-LDH films grown on substrates with different roughness was analyzed by SEM, as shown in Figure 4. It can be clearly seen that all the films have strong adhesion to the substrate and grow densely on the surface of the Mg alloy. The film thickness values of the four samples polished by 600, 1200, 2000, and 5000 sandpaper were 2.2, 2.7, 3.1, and 3.8 µm, respectively. Evidently, the flatter the sample surface, the more uniform the film growth and the greater the thickness value, i.e., the thickness value of the film is negatively correlated with the surface roughness value.

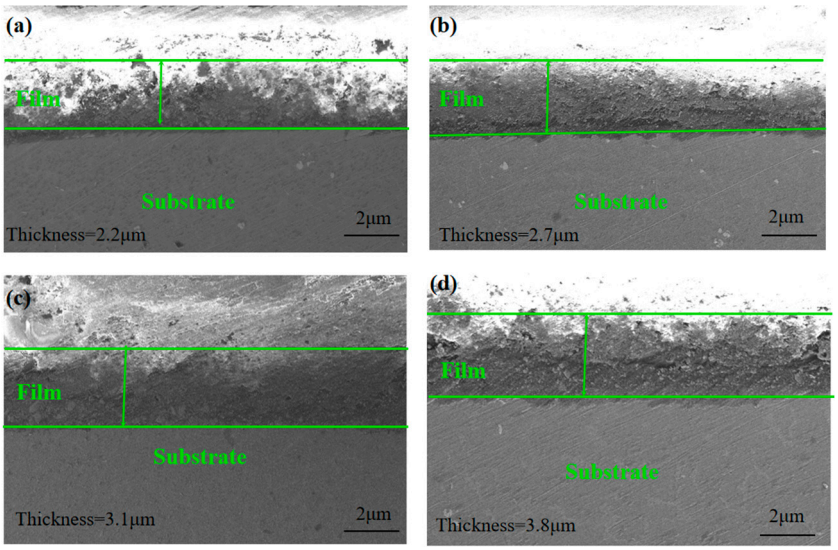


Figure 4. Cross-sectional SEM micrographs of (**a**) 600; (**b**) 1200; (**c**) 2000; (**d**) 5000.

3.5. Wettability Evaluation

Figure 5 shows the water contact angle for bare and ZnAl-LDHs coated samples. The water contact angles of the five samples were 35.92°, 90.85°, 87.23°, 85.06°, and 84.34°,

respectively. The surface hydrophilicity of magnesium alloys was found to be higher than that of LDH films, which was mainly due to the coarseness of the micronanostructures. Surface roughness also affects the hydrophobicity of LDH films. The greater the surface roughness, the greater the water contact angle and the better the hydrophobicity.

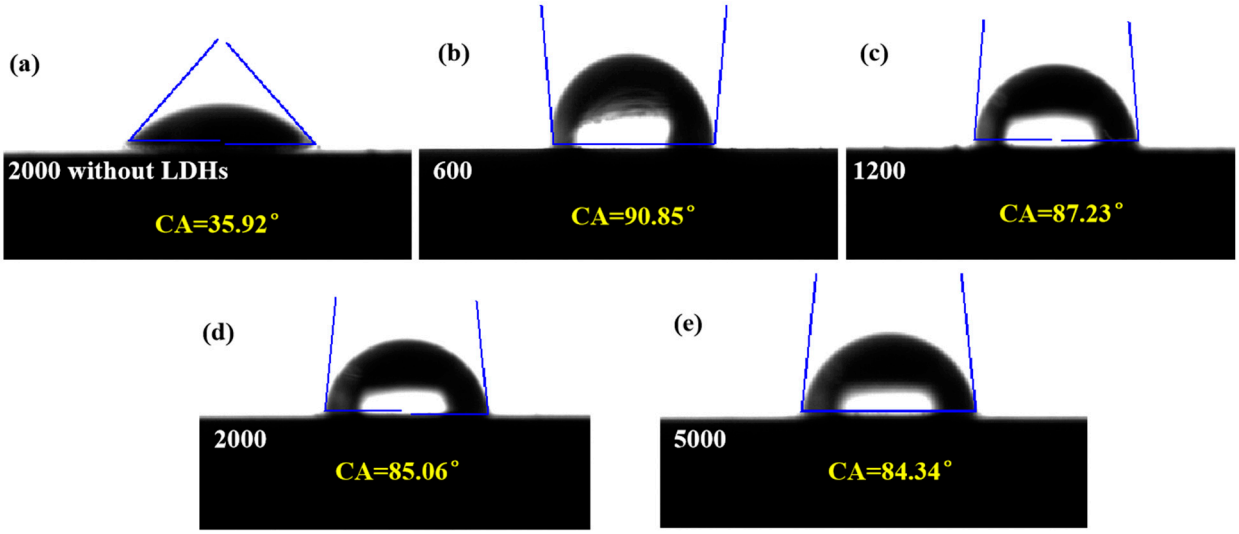


Figure 5. Water contact angle for bare and coated ZnAl-LDHs film samples: (**a**) 2000 (without LDHs); (**b**) 600; (**c**) 1200; (**d**) 2000; (**e**) 5000.

3.6. Binding Force Analysis

To evaluate the adhesion between the ZnAl-LDH films and the magnesium alloy substrates prepared with different roughness, the ZnAl-LDH films were cut and then stripped using a ribbon, as shown in Figure 6. The tapes did not exfoliate the film, indicating excellent adhesion between the film and the substrate.

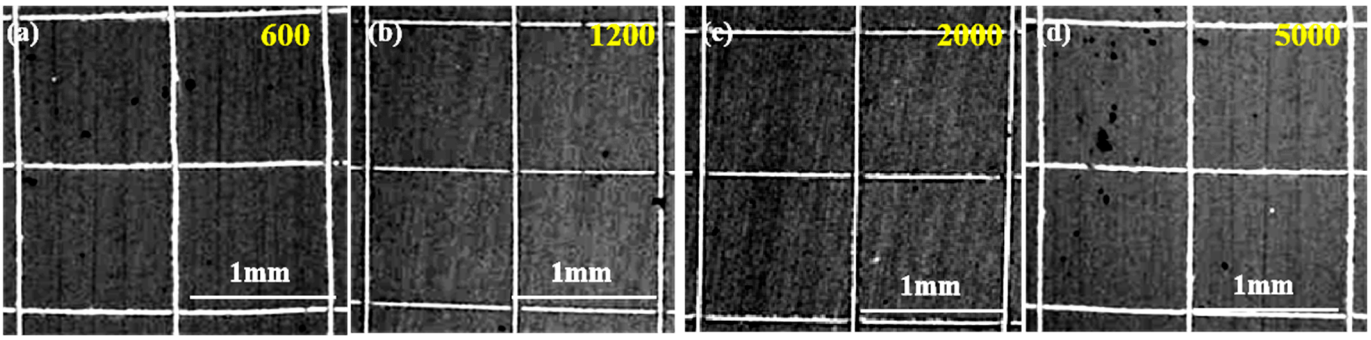


Figure 6. SEM images of ZnAl-LDH films on AZ91D after the tape was peeled off. (**a**–**d**).

3.7. Corrosion Resistance Analysis

3.7.1. Electrochemical Tests Analysis

Figure 7 presents the representative polarization curves of different specimens in 0.1 M NaCl aqueous solution. Using the Tafel extrapolation method, the corrosion current density (i_{corr}) and corrosion potential (E_{corr}) are fitted and summarized in Table 1. Generally, lower E_{cor} and higher i_{corr} values are favorable for thermodynamic and kinetic corrosion. It can be seen that the ZnAl-LDHs film prepared on the magnesium alloy substrate surface polished by the 5000 sandpaper has the highest corrosion potential (E_{corr}). The corrosion current density of the four samples polished by 600, 1200, 2000, and 5000 decreases from 1.24×10^{-3} to 4.13×10^{-4}, 3.19×10^{-4}, and 1.12×10^{-4} A/cm^2. This means that the flatter the surface of the substrate and the lower the roughness the better the corrosion resistance of the LDH films grown on the surface of the sample. For comparison, the corrosion potential

(−1.51 V) and corrosion current (8.81×10^{-3} A/cm^2) of the magnesium alloy substrate with filmless and polished by 2000 sandpaper were also measured and fitted in electrochemical experiments, indicating that the combination of improved surface roughness and the ZnAl-LDH film enhanced the corrosion resistance of the magnesium alloy.

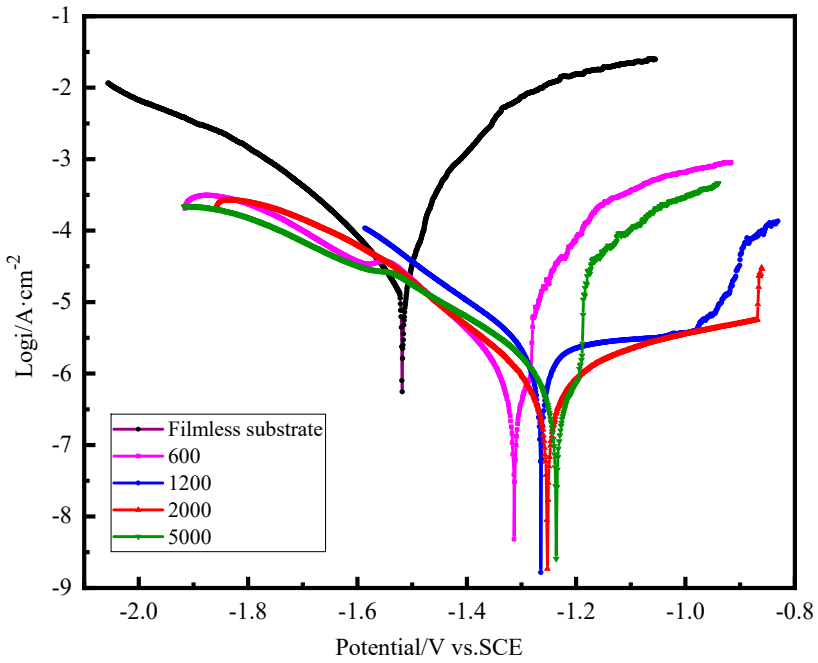


Figure 7. Tafel polarization curves in 0.1 M NaCl solution of ZnAl-LDH films grown on AZ91D Mg alloy with different surface roughness.

Table 1. Corrosion potential (E_{corr}) and corrosion current density (i_{corr}) of different specimens derived from the Tafel extrapolation method.

Specimens	E_{corr} (V_{SCE})	i_{corr} (A/cm^2)
Filmless substrate	−1.51	8.81×10^{-3}
600	−1.32	1.24×10^{-3}
1200	−1.27	4.13×10^{-4}
2000	−1.25	3.19×10^{-4}
5000	−1.23	1.12×10^{-4}

To characterize the protective effect of the thin films on the magnesium AZ91D alloy, the EIS method was employed. It can be seen from Nyquist diagram that the impedance spectrum of ZnAl-LDH film consists of a high-frequency capacitive impedance arc and a low-frequency capacitive impedance arc. The capacitive impedance arc at high frequency is related to the capacitance and resistance of the film layer, whereas the low frequency capacitive impedance arc is related to the capacitance and charge transfer resistance of the electrical double layer. The sample treated with the 5000 sandpaper has the largest impedance radius arc, indicating that it has the best corrosion resistance. The EIS spectra may show one, two, or more time constants depending on the single or multi-layer structure of the films, whether the films are porous or compact, whether the space-charge zone limits the charge transfer forms of the potential used, or the charge transfer process is affected by diffusion. Two well-defined time constants can be seen from Figure 8. The relaxation process at high frequencies is attributed to the porous layer and another low frequency attributes to the internal dense layer. Of these, R_f represents the membrane resistance, R_s represents the solution resistance, R_{ct} represents the membrane-substrate interface, CPE_{dl} describes the double layer capacitance at charge transfer resistance, and CPE_f represents

the capacitance of the bilayer at the interface between the electrode and the electrolyte solution. Electrochemical parameters for the equivalent circuit diagram fitting are shown in Table 2. The thin films of ZnAl-LDHs (600, 1200, 2000, 5000) have transfer resistance fractions of 331.4, 390.3, 424.7, and 512.5 $\Omega \cdot cm^2$, respectively. Thus, the flatter the initial surface is the smaller the roughness is, and the ZnAl-LDH film grown on the surface has a higher charge transfer resistance, i.e., the resistance of the charge flowing through the film to the substrate increases, and the double-layer capacitance of the ZnAl-LDHs film (5000) is the smallest, only 1.78×10^{-6} F/cm^2. Therefore, the ZnAl-LDHs film grown on the surface of the magnesium alloy processed by 5000 sandpaper has the best corrosion resistance on the magnesium alloy.

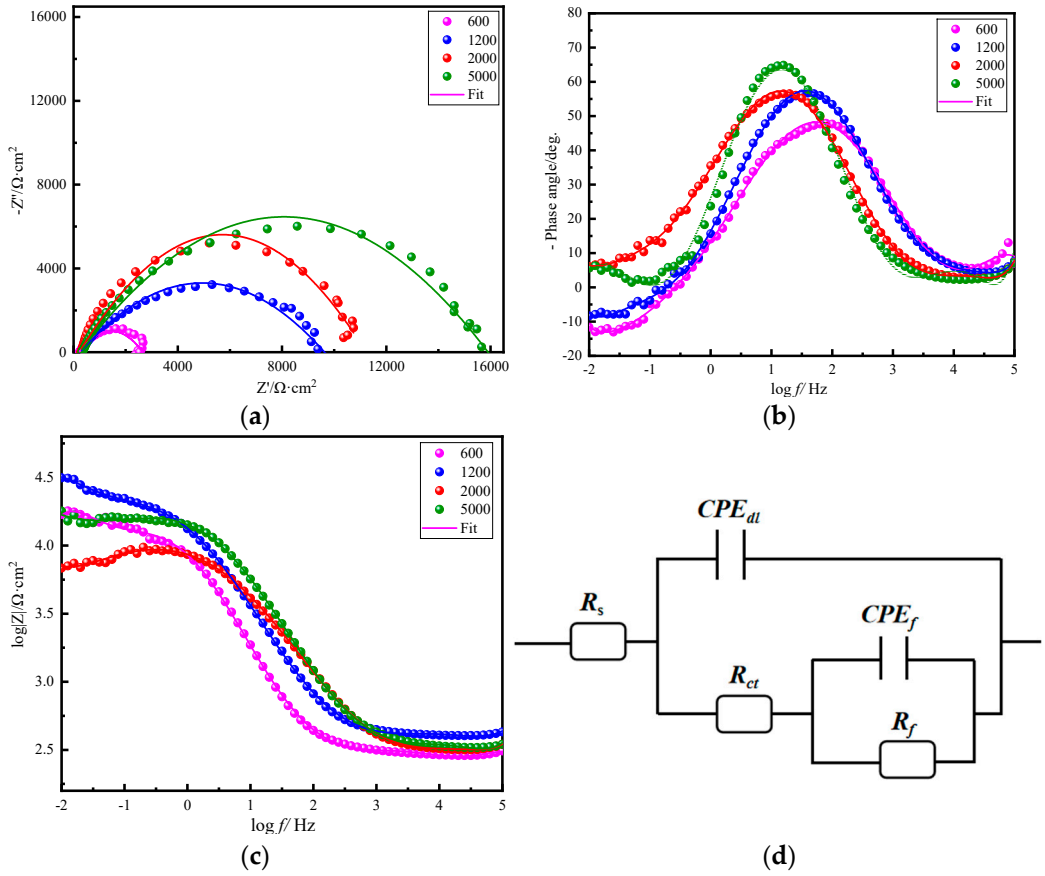


Figure 8. Nyquist diagram (**a**), bode magnitude plots (**b**), bode phase plots (**c**) and equivalent electrical circuit (**d**) of the studied system for ZnAl-LDH films grown on AZ91D magnesium alloy with different surface roughness.

Table 2. Fitting results of the EIS spectrum depicted in Figure 6.

Specimens	R_{sol} ($\Omega \cdot cm^2$)	R_{ct} ($\Omega \cdot cm^2$)	CPE_{dl} ($\mu F\ cm^{-2}$)	R_f ($\Omega \cdot cm^2$)	CPE_f ($\mu F \cdot cm^{-2}$)
600	23.45	331.4	1.15×10^{-5}	153.2	1.78×10^{-5}
1200	21.87	390.3	3.34×10^{-6}	347.8	2.71×10^{-5}
2000	22.49	424.7	2.05×10^{-6}	525.6	1.94×10^{-5}
5000	21.03	512.5	1.78×10^{-6}	932.9	4.62×10^{-5}

3.7.2. Neutral Salt Spray Tests Analysis

The surface corrosion state of the neutral salt spray test of the ZnAl-LDH films grown on AZ91D magnesium alloy with different surface roughness at 0, 6, 24, 48 h is shown in Figure 9. As the neutral salt spray time was extended, white corrosion products appeared on

the surface of each of the samples, and the amount of corrosion products was continuously increased. When the neutral salt spray time reached 48 h, the increased mass of the samples following corrosion gradually decreased as the surface roughness decreased, as can be seen in Figure 10. The sample mass processed by 5000 sandpaper was only increased by 0.0424 g. These results indicated that the surface roughness had a large influence on the corrosion resistance of neutral salt spray. In general, the smaller the surface roughness of the specimens the better the corrosion resistance of the ZnAl-LDHs film that is grown on the surface, and the greater the surface roughness of the specimen the more severe the corrosion resistance. Because of the larger the roughness of the sample surface, condensation is more easily formed on the surface in the salt spray test process, leading to corrosion of the surface. Additionally, the greater the surface roughness the greater the real surface area of the part's surface and the more salt spray contact, thus making it easier to corrode. Simultaneously, in the salt spray test, the smaller the surface roughness of the workpieces the fewer chloride ion residues on the surface and the better the corrosion resistance.

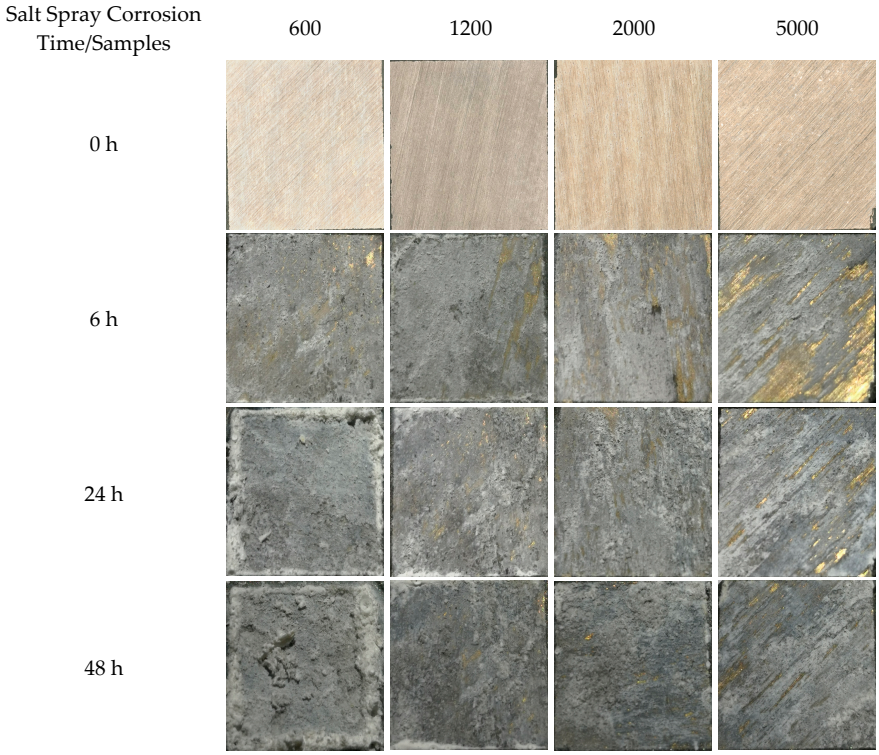


Figure 9. The surface state of the neutral salt spray test of the samples at 0, 6, 24, 48 h.

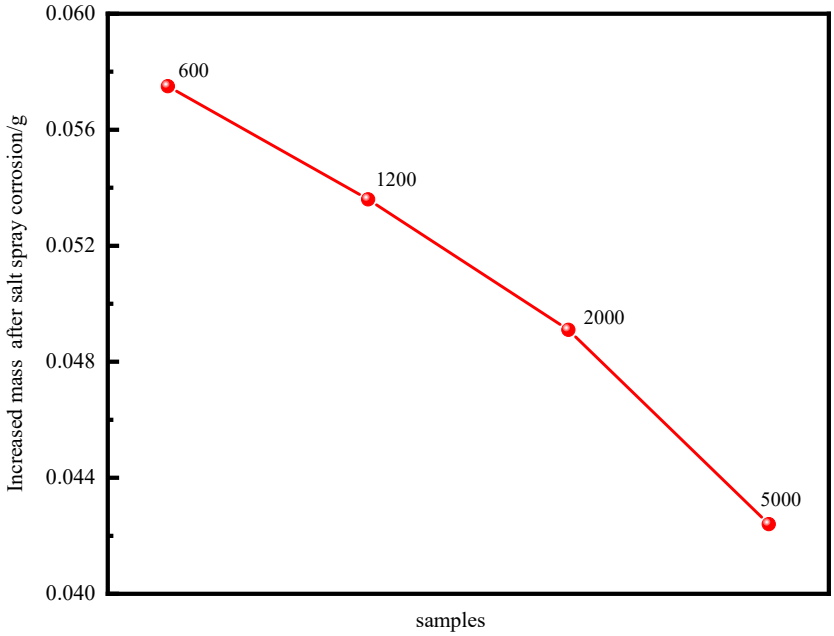


Figure 10. Mass change in samples with different roughness after neutral salt spray corrosion.

4. Discussion

4.1. Mechanism of Thin Film Growth Influenced by Roughness

Although a great deal of work has been performed on the preparation of 2D nano-LDH films, the mechanism of their formation remains controversial. The two accepted growth mechanisms of LDH films are ion substitution theory and dissociation-sediment-diffusion theory. Figure 11 depicts the mechanism of in situ growth of ZnAl-LDH thin film on magnesium alloy surface. Its growth may be consistent with dissociation–sediment–diffusion theory mechanisms [6]. First of all, Al^{3+} and Zn^{2+} react with sodium hydroxide in solution and nucleate uniformly in solution to form metastable intermediate products layered basic aluminum nitrate and basic zinc nitrate crystal nuclei. Then, at a suitable pH, the basic aluminum nitrate and basic zinc nitrate crystal nuclei are adsorbed on the substrate. With the prolongation of crystallization time, ZnAl-LDH grains continue to grow and finally form a staggered nest-like LDH film [27]. The distribution of the LDH nano-sheet formed on the surface of magnesium matrix with high roughness is sparse, and the film thickness is small. On the other hand, the LDH nanoflakes grown on the surface with low surface roughness are uniform in size and compact and thick in thickness. This should be related to the surface bulge of magnesium matrix with high surface roughness. The bulge increases the reaction surface area, and the formed grain boundaries and grain positions are different, which provides more nucleation sites for the growth of LDHs, resulting in differences in the growth speed and direction of the LDH thin film nanoflakes, and thus the film thickness is different everywhere [28,29]. It should be noted that the current formation mechanisms are simplistic. The actual process in an aqueous solution is much more complex and is influenced by the concentration, temperature, pH, and alkalinity of the solution. Therefore, further study of the formation mechanism of LDHs will be an important research topic.

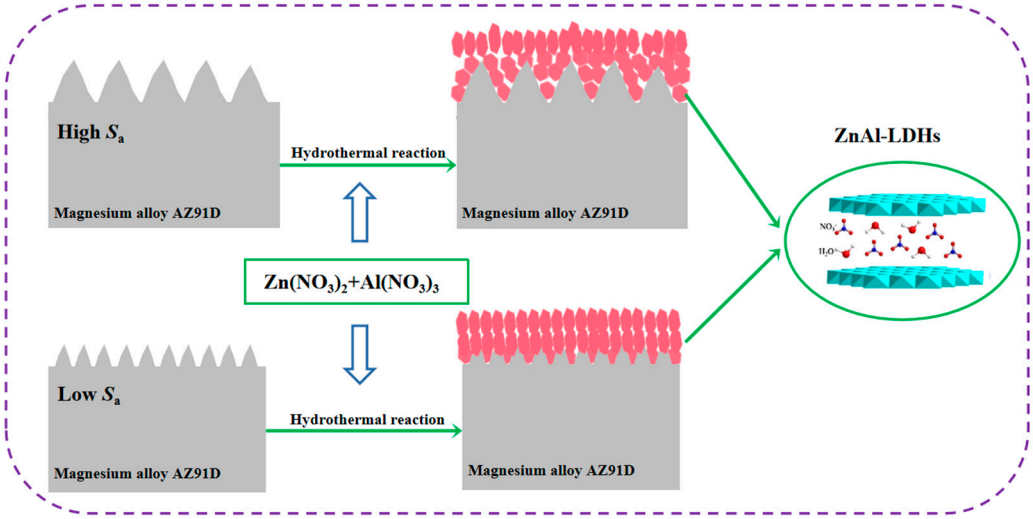


Figure 11. The mechanism of in situ growth of ZnAl-LDHs thin film on magnesium alloy surface.

4.2. Anti-Corrosion Mechanism of ZnAl-LDHs Thin Films

The possible corrosion resistance mechanism for the ZnAl-LDHs film has been proposed: The secretively stacked ZnAl-LDH nano-sheets provide an excellent physical barrier to the corrosive media. In addition, the maze effect [30] of the ZnAl-LDHs film prolongs the corrosion time of the chloride ion to the substrate. The interlaminar anions (NO_3^-) of the prepared ZnAl-LDH nano-sheets acted as chlorine nano-traps. The anion exchange process indicated that LDH could trap corrosive media (Cl^-) and prevent it from contacting the surface of the Mg alloy substrate. Thus, the synergistic effect of the blocking effect, the nano trap effect of chlorine ions, and the labyrinth effect are also responsible for the enhancement of the corrosion resistance of the composite coating [31]. The specific reaction may be expressed as:

$$Al^{3+} + 4NaOH \rightarrow Al(OH)_4^- \quad (1)$$

$$Zn^{2+} + 4OH^- \rightarrow Zn(OH)_4^{2-} \quad (2)$$

$$Zn(OH)_4^{2-} + Al(OH)_4^- + NO_3^- + H_2O \rightarrow ZnAl\text{-}LDHs \quad (3)$$

$$ZnAl\text{-}LDHs\text{-}NO_3^- + Cl^- \rightarrow ZnAl\text{-}LDHs\text{-}Cl^- + NO_3^- \quad (4)$$

5. Conclusions

In this paper, ZnAl-LDH thin films were prepared in situ on magnesium alloys with different surface roughness by hydrothermal method. The following conclusions can be drawn.

(1) The dense ZnAl-LDH films can be prepared on AZ91D magnesium alloys with different roughness by metallographic preparation and subsequent hydrothermal reaction, and the structure of ZnAl-LDH films is tailored by roughness of magnesium alloys.

(2) The smaller the surface roughness, the denser and thicker the ZnAl-LDH films and the better the corrosion resistance and the less the increase in mass after neutralization of salt fog corrosion.

(3) The reason why surface roughness affects the growth rate and direction of LDHs thin film nanosheets may be related to nucleation sites. This also provides a theoretical basis for the optimal processing parameters of magnesium alloy surface.

Author Contributions: Writing—review and editing, X.W.; methodology, K.G.; Investigation, L.Y.; validation, P.L.; writing—original draft preparation, J.H. All authors have read and agreed to the published version of the manuscript.

Funding: This work was supported by Guangdong Major Project of Basic and Applied Basic Research (No. 2019B030302011).

Institutional Review Board Statement: Not applicable.

Informed Consent Statement: Not applicable.

Data Availability Statement: Available upon request from the corresponding author.

Conflicts of Interest: The authors declare no conflict of interest.

References

1. Guo, L.; Wu, W.; Zhou, Y.; Zhang, F.; Zeng, R.; Zeng, J. Layered double hydroxide coatings on magnesium alloys: A review. *J. Mater. Sci. Technol.* **2018**, *34*, 1455–1466.
2. Imandoust, A.; Barrett, C.; Al-Samman, T.; Inal, K.; Kadiri, H. A review on the effect of rare-earth elements on texture evolution during processing of magnesium alloys. *J. Mater. Sci.* **2017**, *52*, 1–29.
3. Hirsch, J.; Al-Samman, T. Superior light metals by texture engineering: Optimized aluminum and magnesium alloys for automotive applications. *Acta Mater.* **2013**, *61*, 818–843. [CrossRef]
4. Ballerini, G.; Bardi, U.; Bignucolo, R.; Ceraolo, G. About some corrosion mechanisms of AZ91D magnesium alloy. *Corros. Sci.* **2015**, *47*, 2173–2184.
5. Cao, F.; Song, G.; Atrens, A. Corrosion and passivation of magnesium alloys. *Corros. Sci.* **2016**, *111*, 835–845.
6. Yan, L.; Zhou, M.; Pang, X.; Gao, K. One-step in situ synthesis of reduced graphene oxide/Zn-Al layered double hydroxide film for enhanced corrosion protection of magnesium alloys. *Langmuir* **2019**, *35*, 6312–6320. [CrossRef]
7. Zhang, G.; Wu, L.; Tang, A.; Zhang, S.; Yuan, B.; Zheng, Z.; Pan, F. A novel approach to fabricate protective layered double hydroxide films on the surface of anodized Mg-Al alloy. *Adv. Mater. Interfaces* **2017**, *4*, 1700163.
8. Gray, J.; Luan, B. Protective coatings on magnesium and its alloys—A critical review. *J. Alloys Compd.* **2002**, *336*, 88–113.
9. Li, Z.; Yang, W.; Yu, Q.; Wu, Y.; Wang, D.; Liang, J.; Zhou, F. A New Method for the corrosion resistance of AZ31 Mg Alloy with porous micro-arc oxidation membrane as ionic corrosion inhibitor container. *Langmuir* **2019**, *35*, 1134–1145. [CrossRef]
10. Wu, F.; Liang, J.; Peng, J.; Liu, B. Electrochemical deposition and characterization of Zn-Al layered double hydroxides (LDHs) films on magnesium alloy. *Appl. Surf. Sci.* **2014**, *313*, 834–840. [CrossRef]
11. Chen, J.; Song, Y.; Shan, D.; Han, E. In situ growth of Mg-Al hydrotalcite conversion film on AZ31 magnesium alloy. *Corros. Sci.* **2011**, *53*, 3281–3288. [CrossRef]
12. Xu, F.; Luo, L.; Xiong, L.; Liu, Y. Microstructure and corrosion behavior of ALD Al_2O_3 film on AZ31 magnesium alloy with different surface roughness. *J. Magnes. Alloys* **2020**, *8*, 480–492.
13. Shao, Z.; Li, P.; Zhang, C.; Wu, B.; Tang, C.; Gao, M. Enhancing the anti-corrosion performance and biocompatibility of AZ91D Mg alloy by applying roughness pretreatment and coating with in-situ $Mg(OH)_2$/Mg-Al LDH. *J. Magnes. Alloys* **2022**, *11*. [CrossRef]
14. Sahin, M.; Çetinarslan, C.; Akata, H. Effect of surface roughness on friction coefficients during upsetting processes for different materials. *Mater. Des.* **2005**, *28*, 633–640. [CrossRef]
15. Yan, X.; Yang, L.; An, Y.; Jin, W.; Li, Y.; Li, B. Surface roughness and hydrophilicity enhancement of polyolefin-based membranes by three kinds of plasma methods. *Surf. Interface Anal.* **2015**, *47*, 545–553.
16. Zhou, M.; Pang, X.; Wei, L.; Gao, K. Insitu grown superhydrophobic Zn-Al layered double hydroxides films on magnesium alloy to improve corrosion properties. *Appl. Surf. Sci.* **2015**, *337*, 172–177.
17. Yan, Q.; Yang, K.; Wang, Z.; Chen, M.; Sun, G.; Ni, Z. Surface roughness optimization and high-temperature wear performance of H13 coating fabricated by extreme high-speed laser cladding. *Opt. Laser Technol.* **2022**, *149*, 107823. [CrossRef]
18. Gao, Y.; Sun, Y.; Guo, D. Facile fabrication of superhydrophobic surfaces with low roughness on Ti-6Al-4V substrates via anodization. *Appl. Surf. Sci.* **2014**, *314*, 754–759. [CrossRef]
19. Borkowski, M.; Mazur, Ł.; Maćkosz, K.; Mazur, T.; Szuwarzyński, M. Low roughness, elevated stiffness and thickness modulated surface nanocomposites based on the controlled deposition of polystyrene nanoparticles. *J. Mater. Res. Technol.* **2022**, *19*, 2799–2809. [CrossRef]
20. Durst, O.; Ellermeier, J.; Berger, C. Influence of plasma-nitriding and surface roughness on the wear and corrosion resistance of thin films (PVD/PECVD). *Surf. Coat. Technol.* **2008**, *203*, 848–854. [CrossRef]
21. Chen, J.; Song, Y.; Shan, D.; Han, E. Study of the corrosion mechanism of the in situ grown Mg-Al-CO_3^{2-} hydrotalcite film on AZ31 alloy. *Corros. Sci.* **2012**, *65*, 268–277. [CrossRef]
22. Pancrecious Jerin, K.; Gopika, P.; Suja, P.; Ulaeto, S.; Gowd, E.; Rajan, T. Role of layered double hydroxide in enhancing wear and corrosion performance of self-lubricating hydrophobic Ni-B composite coatings on aluminium alloy. *Colloids Surf. A* **2022**, *634*, 128017. [CrossRef]

23. Zhou, M.; Yan, L.; Ling, H.; Diao, Y.; Pang, X.; Wang, Y.; Gao, K. Design and fabrication of enhanced corrosion resistance Zn-Al layered double hydroxides films based anion-exchange mechanism on magnesium alloys. *Appl. Surf. Sci.* **2017**, *404*, 246–253. [CrossRef]
24. Li, J.; Bian, Y.; Tu, X.; Li, W.; Song, D. Influence of surface roughness of substrate on corrosion behavior of MAO coated ZM5 Mg alloy. *J. Electroanal. Chem.* **2022**, *910*, 116206. [CrossRef]
25. Wang, X.; Gao, K.; Yan, L.; Yang, H. Effect of 2D Nanocrystalline ZnAl-LDHs Films with Different Orientations on Anticorrosion Performance of Magnesium Alloys. *Mater. Lett.* **2021**, *293*, 129708. [CrossRef]
26. Bunch, J.; Verbridge, S.; Alden, J.; Van, A.; Parpia, J.; Craighead, H.; Mceuen, P. Impermeable atomic membranes from graphene sheets. *Nano Lett.* **2008**, *8*, 2458–2462. [CrossRef]
27. Chen, Y.; Yao, W.; Wu, L.; Chen, J.; Pan, F. Effect of Microstructure on Layered Double Hydroxides Film Growth on Mg-2Zn-xMn Alloy. *Coatings* **2021**, *11*, 59. [CrossRef]
28. Wang, Y.; Huang, Q.; Zhou, B.; Yuan, Z.; Wei, Y.; Fujita, T. Corrosion Protection of 6061 Aluminum Alloys by Sol-Gel Coating Modified with ZnLaAl-LDHs. *Coatings* **2021**, *11*, 478. [CrossRef]
29. Wen, S.; Wang, X.; Ren, Z. Microstructure and Corrosion Resistance of an HVAF-Sprayed Al-Based Amorphous Coating on Magnesium Alloys. *Coatings* **2022**, *12*, 425. [CrossRef]
30. Chen, Y.; Wu, L.; Yao, W.; Zhong, Z.; Chen, Y.; Wu, J.; Pan, F. One-step in situ synthesis of graphene oxide/MgAl-layered double hydroxide coating on a micro-arc oxidation coating for enhanced corrosion protection of magnesium alloys. *Surf. Coat. Technol.* **2021**, *413*, 127083. [CrossRef]
31. Saji, V.S.; Narayanan, T.S.; Chen, X. *Conversion Coatings for Magnesium and Its Alloys*; Springer International Publishing: Berlin/Heidelberg, Germany, 2022; pp. 211–243.

Disclaimer/Publisher's Note: The statements, opinions and data contained in all publications are solely those of the individual author(s) and contributor(s) and not of MDPI and/or the editor(s). MDPI and/or the editor(s) disclaim responsibility for any injury to people or property resulting from any ideas, methods, instructions or products referred to in the content.